Available online at www.sciencedirect.com
ScienceDirect
Polymer 48 (2007) 2818–2826
polymer
www.elsevier.com/locate/polymer

Surface segregation of branched polyethyleneimines in a thermoplastic polyurethane

Joshua A. Orlicki, Wendy E. Kosik, J. Derek Demaree, Matthew S. Bratcher, Robert E. Jensen, Steven H. McKnight*

Rodman Materials Research Center, Multifunctional Materials Branch, Army Research Laboratory, AMSRD-ARL-WM-MA, 4600 Deer Creek Loop, Aberdeen Proving Ground, MD 21005-5069, United States

Received 17 November 2006; received in revised form 6 March 2007; accepted 8 March 2007
Available online 13 March 2007

Abstract

Hyperbranched polyethyleneimines were modified with methacrylated fluorosurfactants and aliphatic epoxides to provide a library of macromolecules with controlled chain ends and residual amine functionality. These materials were co-dissolved with a thermoplastic polyurethane-ether and the blends were subsequently deposited as films cast from solution. The surface chemistry of the cast films was determined using angle resolved X-ray photoelectron spectroscopy (AR-XPS) and Rutherford backscattering spectroscopy (RBS). Experimental results indicate that the modified hyperbranched polymers (HBPs) concentrate at the air–polymer interface. Furthermore, HBPs that were complexed to polyoxometalates (POMs) using electrostatic interactions also exhibited surface segregation in cast polymer films, resulting in ca. 10-fold increase of metal at the film surface relative to the known bulk concentration. Results from XPS and RBS examination of the films are consistent with surface segregation of the HBP–POM hybrids, exhibiting increased metal, fluorine, and nitrogen content near the surface of the film, as well as significant changes in wetting behavior. This study indicates that modified HBPs may be used to selectively transport inorganic species such as polyoxometalates to polymer film surfaces.

Keywords: Hyperbranched polymer; Surface segregation; Polyoxometalate

1. Introduction

Polymers containing perfluorinated backbones or side chains are known to migrate to polymer surfaces and control polymer surface energy [1]. Previous research has demonstrated that the incorporation of perfluorinated small molecules into linear low-density polyethylene [2] increased the hydrophobicity of the extruded film surface substantially, and the surface composition of the blend confirmed migration of the small molecule additive. Similar results were obtained for surface modifying macromolecules (SMMs) blended into poly(ether-sulfone). The chain-end perfluorinated polyurethane SMMs were found to migrate to the surface of cast films more efficiently at longer drying times, allowing the surface of the films to be controlled based upon SMM incorporation and drying/cure rates [3]. The behavior of larger molecules has also been studied. Koberstein and coworkers have extensively studied the effects of perfluorination on the miscibility and migration properties of perfluoro-terminated polymer films [4,5]. In a PS system, as the chain length increased, the ability of perfluorinated chain ends to migrate to the surface decreased [1]. Kajiyama and coworkers observed similar results when examining α,ω-fluoroalkyl terminated PS chains of varying molecular weight. In addition to finding that fluoro-alkane organization was dependent on the PS molecular weight in samples annealed under vacuum, they found that annealing the films in boiling water resulted in surface depletion of the perfluorinated chains [6], illustrating the importance of environmental conditions

* Corresponding author.
E-mail address: shm@arl.army.mil (S.H. McKnight).

0032-3861/$ - see front matter © 2007 Published by Elsevier Ltd.
doi:10.1016/j.polymer.2007.03.021

upon the ultimate surface composition. Ward and Long had demonstrated a similar type of environmental response using central functionalized triblock copolymers [7]. The polymers were grafted onto a substrate via the central block, and then their properties could be controlled based upon solvophobic/solvophilic driving forces. Similar selective surface migration has also recently been demonstrated using diblock copolymer brushes grafted onto silica substrates [8].

Dendritic polymers, including both dendrimers and less precise hyperbranched polymers (HBPs), are a widely studied class of materials that can be synthesized to possess good solubility in a variety of solvents and high functional group density [9–11]. These characteristics have enabled the development of dendrimer-based phase transfer agents [12], especially useful for promoting metal transport into supercritical CO_2 phases using perfluoro-chain modified macromolecules [13]. Dendritic materials, by virtue of their low viscosity and plurality of end groups, may hold great promise for designing surface segregating additives which optimize the influence of perfluorinated chains while maintaining the desirable properties of the core polymer. Indeed, the behavior of many dendrimer and hyperbranched polymer additives has been studied in the literature [14,15]. Hyperbranched polymers (HBPs) maintain a high density of reactive chain ends and exhibit good solubility, yet sacrifice perfect branching or narrow polydispersities for their synthetic accessibility. End-group functionalization has led to HBP/linear polymer blends that exhibited increased fluorine levels at the surface and changes in surface contact angle with water [16]. Dendritic materials have also been used to encapsulate dye molecules in melt processed polyolefins [15], or to modify their flow properties during extrusion or blow-molding [17]. These studies and others have shown that many of the beneficial attributes of dendrimeric materials may be accessed with the hyperbranched polymer structure.

The research detailed herein investigates the surface segregation of end-group modified HBPs in solution cast polymers as well as the surface segregation of HBP–inorganic conjugates. Specifically, the segregation of commercially available polyethyleneimine HBPs that have been conjugated to polyoxometalates (POMs) has been examined. While POMs have been used to form hybrids with dendritic structures previously [18], this is the first instance where a dendritic material has been used to enhance their surface segregation in a polymer film.

2. Experimental procedures

2.1. Materials

Commercially available highly branched polyethyleneimines (PEIs) were provided by BASF Corporation. The PEI investigated for this work was Lupasol G20WF (water-free), with an average molecular weight of 1300 Da and 1°:2°:3° amine ratio of 1.0:0.91:0.64 (data from BASF, equivalent weight ca. 110 g/1° amine). DuPont Corporation provided Zonyl TM, a methacrylated perfluorinated surfactant (mixture of perfluoro segment chain lengths, range from C_4–C_{20}, greatest populations of C_6 and C_8 length. For stoichiometric calculations, used average MW = 532, mass of C_8 chain length). A reactive aliphatic epoxy was provided by Resolution Performance Products (Heloxy 8, mixture of chain lengths, average MW 288). Thermoplastic polyurethane (TPU) was provided by Noveon (Estane 58237). Polyoxometalates were received from Professor Craig Hill at Emory University. All other chemicals and solvents were obtained from Alfa-Aesar and were used as received.

2.2. Characterization techniques

Infrared spectroscopy was performed using a Spectrum 2000 FT-IR spectrometer from Perkin–Elmer. Films were cast on 25 mm NaCl plates from THF, and recorded under absorbance mode (64 scans, 2 cm^{-1} resolution). Nuclear magnetic resonance spectroscopy was carried out using a Bruker-Biospin 600 MHz Ultrashield Avance spectrometer, equipped with a standard bore broadband probe (5 mm OD tubes, 32 scans, 5 s d1). Spectra were obtained in $CDCl_3$ at room temperature, and all resonances are reported as ppm referenced to the residual solvent peak (δ 7.26 ppm).

2.3. Surface characterization

Contact angles were recorded using a goniometer equipped with a digital camera and an image capture program employing LabView software. Contact angles were measured using HPLC grade water by defining a circle about the drop, and recording the tangent angle formed at the substrate surface.

Near surface compositional depth profiling was performed using the Kratos Axis 165 X-ray photoelectron spectroscopy system, equipped with a hemispherical analyzer. A 100 W monochromatic A_1 Kα (1486.7 eV) beam irradiated a 1 mm × 0.5 mm sampling area. Angle resolved X-ray photoelectron spectroscopy (AR-XPS) was utilized with data acquired at 30° and 90° take-off angles (TOA, depth of analysis ca. 5 nm and 10 nm, respectively). Shallow TOAs accentuate the spectral contributions of any component that has segregated to the surface. Survey scans were taken at pass energy = 80 eV. Elemental high resolution scans for C 1s, O 1s, N 1s, and F 1s were taken at pass energy = 20 eV. Kratos' Vision 2 software was utilized for all data analysis, linear background subtraction, curve fitting, peak integration, and charge compensation.

The Rutherford backscattering spectroscopy (RBS) experiments were performed using 2 MeV He^+ ion beams from an NEC 5SDH-2 tandem positive ion accelerator. The backscattering angle was 170° and the solid angle of the surface barrier detector was approximately 4 msr. When it was necessary to enhance the depth resolution, the samples were tilted with respect to the beam in an ''IBM'' configuration: the surface normal coplanar with the incoming ion beam and the direction of the scattered ions. All spectra were fit and interpreted using the program RUMP [19].

2.4. Film preparation

Samples for RBS, XPS, and contact angle analysis were prepared by creating stock solutions of known concentration

of matrix polymer (~30 mg/mL) and HBP (~10 mg/mL) in THF. The solutions were combined to provide samples with the desired relative concentrations, metered out with automatic repipettors and confirmed with gravimetric monitoring. Samples were prepared with a varied amount of additive content on a solids wt/wt basis compared to the bulk matrix (Estane 58237 TPU, a segmented polyurethane-ether with soft segments of polyethylene glycol). Films were cast on Si wafers or glass microscope slides that had been cleaned with methanol and acetone. The films were dried at room temperature under covered petri dishes to slow the rate of evaporation and minimize drying defects. Smooth, defect-free films were obtained using these procedures.

A similar process was used for the preparation of HBP–POM hybrids, where a stock solution of polyoxometalate was prepared in the desired solvent. The $H_5PV_2Mo_{10}O_{40}$ and $Na_5PV_2Mo_{10}O_{40}$ POMs were soluble in THF. The Mo-based POMs formed an insoluble green precipitate with the HBP. If the precipitate-containing solution was acidified with sufficient HCl to account for the 1°, 2°, and 3° amines in the HBP backbone, then the precipitate dissolved and a soluble complex was obtained.

2.5. Representative synthetic procedure (HBP **5**)

A 40 mL screw top vial was charged with hyperbranched polyethyleneimine (PEI, 2.01 g, ~18.4 mmol 1° amine equiv.) followed by methacrylated fluorosurfactant (1.01 g, 1.9 mmol). The two fluids were mixed vigorously using a vortex mixer, and were then placed in a heating block set to 60 °C. The vial was removed periodically (every ca. 15 min) and agitated for ca. 20 s with a vortex mixer. After 3 h a waxy liquid had formed and an aliphatic epoxy (1.68 g, 5.9 mmol) was added to the vial and the mixture was agitated as indicated (e.g. vortex mixer, 20 min intervals). After heating for an additional 2.5 h, the vial was removed from the heating block and was placed in a refrigerator (slow ester displacement to form amides at room temperature led to crosslinked product after several months, which was minimized by storage at reduced temperatures). The polymer formed an yellow viscous oil. The polymers were analyzed and used without further purification. ^{1}H NMR (600 MHz, $CDCl_3$, δ): 3.60–3.30 (5H, from aliphatic additive), 2.71, 2.64, 2.58, 2.50, 2.46 (contribution from $-CH_2CH_2NH-$ backbone, 27H), 1.48 (2H), 1.18 (16H), 0.80 (3H). ^{13}C NMR (150 MHz, $CDCl_3$, δ): 71.6, 71.5, 54.3, 54.2, 52.9, 52.3, 49.2, 47.4, 41.5, 39.7, 31.7, 29.5, 29.2, 26.0, 22.5, 14.0, 13.9 ($-CH_3$).

3. Results and discussion

3.1. Synthesis

The route employed for the modification of hyperbranched polyethyleneimines (PEIs) is shown Scheme 1. The methacrylate moieties of the fluorosurfactants were reacted via Michael addition to the amine termini of the polyethyleneimine. The extent of conversion was monitored by FT-IR spectroscopy, as the carbonyl absorbance of the fluorosurfactant shifted from 1728 cm^{-1} to 1739 cm^{-1} upon the consumption of the methacrylate group. The reaction required ca. 3 h to reach completion at 60 °C. Polymers **1**–**4** were prepared with increasing amounts of fluorosurfactant (10 wt% for **1**, 20 wt% for **2**, etc.). The resultant materials were translucent pastes with a slight yellow tinge (indicating a low level of amine oxidation). Compositional data for the polymer series are presented in Table 1.

Polymer **5** was prepared beginning with the fluorosurfactant end-group substitution intermediate between HBPs **3** and **4** (0.1 mol fraction, based on 1° amine chain ends), and was subsequently reacted with an aliphatic epoxy. The epoxy

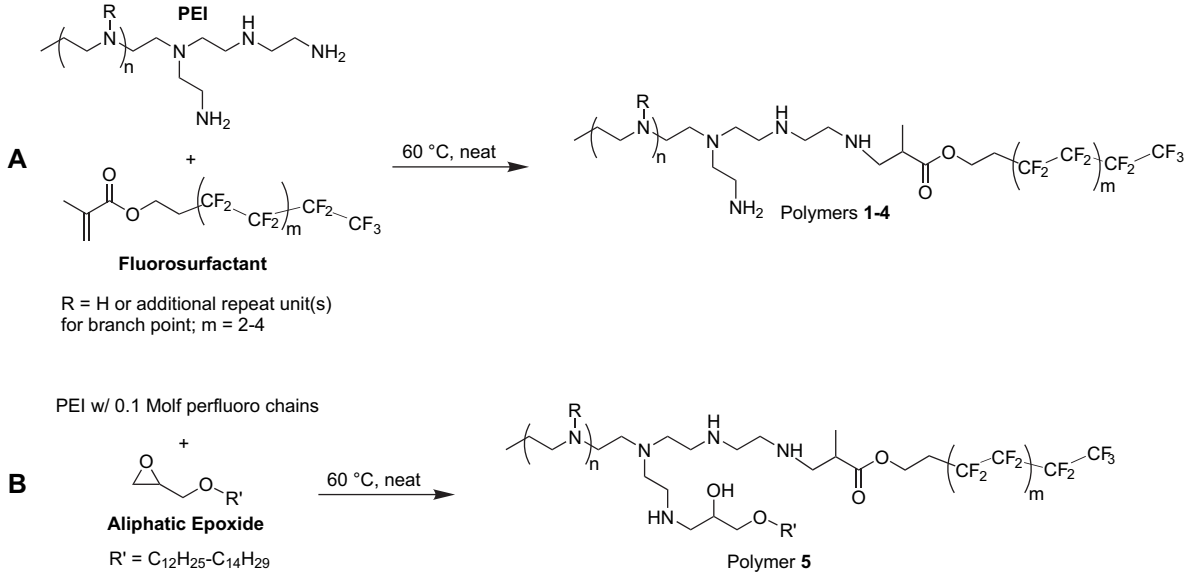

Scheme 1. Methods of PEI modification. Note: structure of PEI is representative and provides examples of chain ends (1° amines), linear segments (2° amines), and branch points (3° amines). Route A: neat Michael addition of methacrylate to amine end groups. Route B: epoxy ring-opening by amine end groups.

Table 1
Composition of HBP end groups

	Polymer	1	2	3	4	5
End group	W_f fluoro	0.1	0.2	0.3	0.4	0.22
	Mol_f fluoro	0.023	0.052	0.089	0.139	0.10
	W_f aliphatic	–	–	–	–	0.35
	Mol_f aliphatic	–	–	–	–	0.45

W_f = weight fraction of end group as a function of total component mass; Mol_f = mole fraction of end groups consumed, relative to 1° amine chain ends.

was added to the reaction mixture after the fluorosurfactant was fully consumed, and required an additional 2.5 h of incubation at the same reaction temperature. Examination of polymer **5** by ^{1}H NMR confirmed the consumption of the epoxy group, as the individual resonances from the epoxy ring system (δ 3.68, 3.47, 3.36 ppm) shifted to two broad peaks after reaction onto the HBP scaffold (δ 3.82, broad signal at 3.38–3.35 ppm). Analysis with FT-IR also indicated the disappearance of the characteristic epoxy absorption at 915 cm^{-1}, and the –OH peak resulting from the epoxy ring-opening intensified and broadened the amine peaks arising from the polymer backbone. Polymers **1**–**4** showed similar characteristics by both ^{1}H and ^{13}C NMR. In the ^{1}H spectrum, the samples exhibited weak, broad signals at ca. 3.3 ppm and 2.0 ppm, and the methyl group at 0.84 ppm resulting from the aliphatic portions of the fluorosurfactant methacrylate. The low mole fraction of fluorosurfactant incorporated into these polymers coupled with intense C–F coupling constants translated into minimal change in ^{13}C spectrum. The methyl and carbonyl groups of the fluorosurfactant were observed as well resolved but weak signals, at 16.0 ppm and 175.7 ppm, respectively. The modified HBPs were used for film preparation without further purification.

The PEI-fluorosurfactant polymers (**1**–**4**) had limited solubility in common organic solvents (e.g. THF, CH_2Cl_2), which decreased as the fluorine content increased. Polymer **5** exhibited improved solubility in these solvents due to the aliphatic chains attached to the core. Solubility remained good for all polymers in binary solutions of THF and water or methanol. The determination of molecular weight for these materials was difficult due to their highly amphiphilic nature and the resultant shift in solubility as the fraction of perfluorinated segments increased. Absolute molecular weight evaluation using multi-angle laser light scattering was attempted, but aggregation occurred at very low concentrations in several solvent systems.

3.2. HBP polymer blend cast films

The physical properties of HBP-based materials are known to be poor due to ineffective chain entanglement formation. When blended with linear polymers, the lack of chain entanglements permits efficient migration of the HBPs to the air interface of the bulk polymer system. The bulk material selected was a commercially available linear polymer, a thermoplastic polyurethane (TPU). It was selected as a proxy for candidate materials used in the preparation of nonwoven membranes with moisture transport properties of interest to the Army [20]. The influence of end-group composition on additive migration performance was isolated by maintaining the HBP core constant across the library of prepared materials. The thermodynamic driving force for segregation was adjusted by controlling the average degree of conversion of the HBP end groups into perfluorinated chains.

To determine the influence of substituting perfluorinated chain ends on the amine termini of the HBP core, a series of TPU/HBP solutions were prepared with progressively increasing HBP loading in the TPU matrix. Here, the term loading is used throughout to refer to the amount of additive in the films; the term substitution is used exclusively to describe the extent (mole fraction) of end-group modification of the HBP chain ends. Films were cast from the solutions onto glass microscope slides. The polymer solutions were dried slowly in an enclosed space (e.g. inside a small petri dish) to provide an environment saturated with solvent vapor. This precaution generated thick films (tens of μm) with reduced drying defects. The samples were analyzed using both contact angle analysis and AR-XPS.

Table 2 details the results of the AR-XPS study undertaken to evaluate these blended films at the indicated loading levels. For a baseline comparison, the theoretical average composition of C, F, and N was calculated for each film based on

Table 2
AR-XPS elemental composition of TPU films at indicated TOA and loading

Additive	F					N				
	Thr. Bulk	0.5%		5.0%		Thr. Bulk	0.5%		5.0%	
		90°	30°	90°	30°		90°	30°	90°	30°
TPU	0.00	0.00	0.00	0.00	0.00	2.04	2.04	0.93	2.04	0.93
PEI	0.00	0.00	0.00	0.00	0.00	3.53	2.46	1.93	3.94	3.18
HBP **1**	0.23	0.40	0.86	2.57	4.78	3.38	2.54	1.75	4.98	4.54
HBP **2**	0.45	0.76	2.83	6.95	10.27	3.24	4.06	3.32	8.44	5.71
HBP **3**	0.68	3.46	6.99	9.02	14.22	3.09	4.26	4.08	8.90	7.47
HBP **4**	0.90	5.36	10.27	14.00	20.19	2.95	4.46	3.39	8.67	7.90
HBP **5**	0.48	2.92	8.22	5.75	13.11	2.63	7.85	6.67	7.09	6.47

Composition of the films was determined for each element (F or N) at the indicated take-off angle (TOA, either 90° or 30°) and at the indicated loading of the TPU film (0.5 wt% or 5.0 wt%). Sampling depth at 90° TOA is ca. 10 nm and ca. 5 nm at 30° TOA. Each value is normalized to the carbon content of the sample, representing a ratio of the total integrated value for the given nucleus over the total carbon signal. The column labeled "Thr. Bulk" indicates the calculated bulk composition based on observed TPU elemental composition with 5% loading of additive.

5% additive in the TPU. This value (column labeled Thr. Bulk in Table 2) should be compared to the observed surface composition, as it accounts for the influence of the additive on the formulation assuming uniform distribution. The samples containing fluorine exhibited an increased atomic abundance at the 30° TOA relative to the 90° TOA. This indicates stratification in the top ca. 10 nm of the surface, with the perfluoro chains residing most prominently at the air–polymer interface. These changes are illustrated further in Fig. 1, which shows the C1s spectra for samples with 5.0% additive loading. In the absence of the perfluoro chains, the PEI does not modify the surface composition significantly. With proper end-group modification, however, the HBPs shift the prominent C1s peak to 286 eV and the signal for the C–F bonding structure arises near 292 eV. The ability of the perfluorinated end groups to transport the HBP core to the film surface is illustrated in Fig. 2. The N 1s intensities were plotted for a film of the base TPU, as well as films with 5% loading of the unmodified PEI, polymer **4**, and polymer **5**. The characteristic shape of the TPU nitrogen signal is unperturbed when the unmodified PEI was the only additive. The new nitrogen signal observed for the modified HBPs, however, is indicative of the PEI core transported to the surface of the film due to the segregation of the perfluorinated segments.

In every instance, the increase in perfluoro-chain substitution on the HBP chain ends led to increased F content at the surface, along with a corresponding increase of observed N abundance. In most cases there was a marked compositional difference between the 0.5% and 5.0% loading levels, though this difference appeared to be minimized for HBP **5**. The TPU films containing the mixed end-group HBP exhibited comparable nitrogen and fluorine abundance for both loading levels. The convergence of elemental composition at both the 0.5% and 5.0% loading levels is also reflected in the behavior of HBP **5** blends when contact angle is used as a metric.

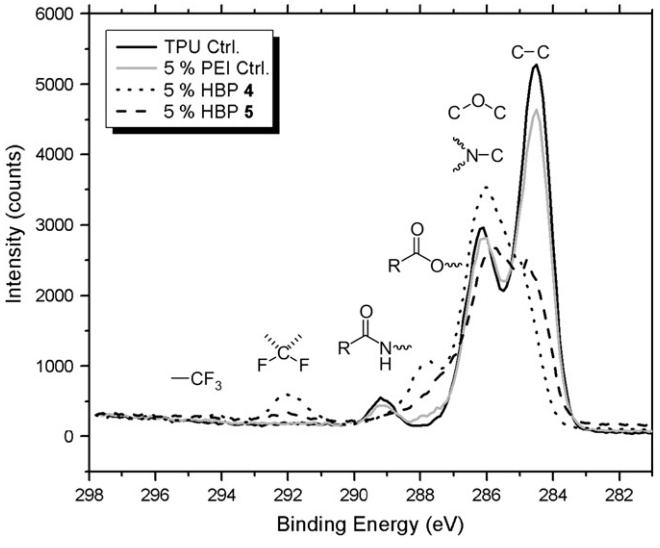

Fig. 1. High resolution C 1s XPS (90° TOA) of 5% additive in TPU films. Little difference observed in C 1s binding between TPU and PEI-loaded samples. A substantial shift is observed with the efficient-migrating HBPs added to the matrix, resulting in greater signal at ca. 286 eV. Prominence of CF binding energies observed at ca. 292 eV for HBP **4** and to a lesser extent HBP **5**. Note: intensities normalized at 297.8 eV, aliphatic C 1s peak shifted to 284.5 eV.

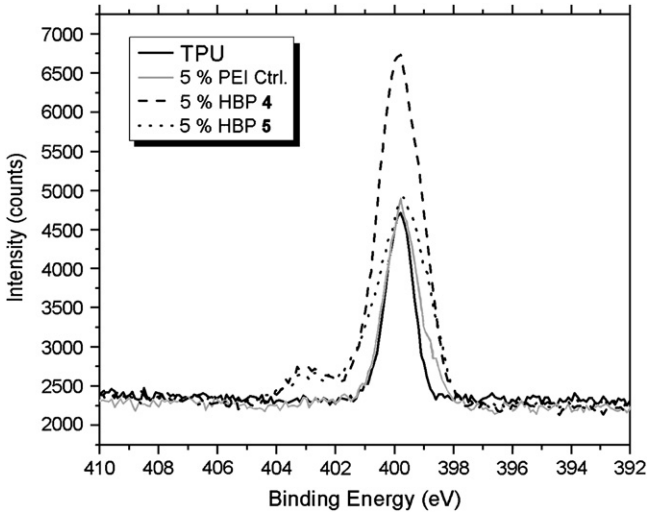

Fig. 2. High resolution N 1s XPS (90° TOA) of 5% additive TPU matrix films. Minimal influence of 5% PEI on nitrogen signal. A new signal was observed with the efficient-migrating HBPs added to the matrix, located at ca. 403 eV. Signal likely arising from aliphatic C–N bonding from HBPs **4** and **5**; the TPU signals are predominantly urethane linkages at ca. 400 eV.

The contact angles of the films with loading levels ranging from 0.5% to 5.0% are shown in Fig. 3. Due to the hydrophilic nature of the base PEI hyperbranched core, the addition of the modified HBPs was expected to reduce the water contact angle of the blends by an amount corresponding to the local surface

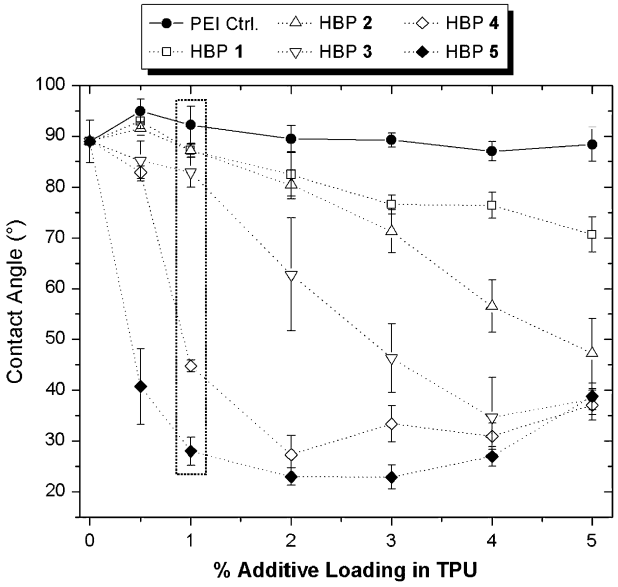

Fig. 3. Advancing contact angle (H_2O) correlated with additive loading. Evaluation of contact angle (surface energy) of TPU blends with the indicated weight fraction of additive. Note that high levels of HBP modification result in substantially improved migration at low concentrations, and the minimal change observed with unmodified HBP–PEI. Box highlights 1% loading samples, demonstrating improved surface migration as end-group substitution increases. Bars indicate one standard deviation from a minimum of five measurements.

concentration of the PEI. The blends containing unmodified PEI exhibited essentially no change in contact angle, while HBP **5** had the greatest influence, especially at the lowest loading level. The extent of contact angle change observed in the blends corresponds to the extent of end-group substitution. Consider the data points boxed in Fig. 3, which highlight the behavior of the films at 1.0% loading. As the level of fluorosurfactant substitution increases, the contact angle of the film decreases. HBP **5** exhibited the greatest influence on contact angle at this loading level, as the mixed chain ends maximized the surface segregation of the HBP.

The data shown in Table 1 and Fig. 3 appear contradictory. The XPS results show increases in surface concentration of fluorocarbon species which intuitively should increase water contact angle, yet the contact angle measurements clearly indicate an increase in the hydrophilicity of the samples containing fluoro-modified HBPs. One reason for the observed behavior may be attributed to the highly globular nature of HBPs and the resulting mobility of the branch segments. The hydrophilic core of the HBP molecule is in close proximity to the chain ends and rapid local molecular rearrangements induced by the presence of water during contact angle analysis could lead to the observed hydrophilic surface. Otherwise stated, the HBPs rearrange rapidly during the environmental exposure to water and the increased presence of the modified HBPs with hydrophilic cores results in the observed contact angle behavior. Indeed the increased surface concentration of nitrogen in these samples corresponds to the measured decrease in contact angle.

The results presented here clearly demonstrate that the modified HBPs segregate at the air–polymer film surface in these HBP/TPU blends. Additional research is necessary to fully elucidate the complex mechanisms that are responsible for the observed behavior. For example, thermoplastic polyurethanes exhibit microphase segregation and the effect of the HBP additive on phase separation behavior and the potential for preferential association of the modified HBPs in the microphase domains were not examined here. The incorporation of perfluoro chains in polyurethane hard segments has been shown to reduce phase segregation in polyurethane ethers [21], but the influence of perfluoro-containing additives is less clear. Unfortunately, the techniques used to probe the properties of the film do not possess the spatial resolution necessary for the assessments and are reliable to sample relatively large surface areas when compared to the domain sizes typical of polyurethanes, and these measurements reflect the aggregate surface properties of the modified polymer. Additional detailed research is required to delineate the complex mechanisms that govern phase segregation and surface segregation in these systems. Other parameters for study include solvent choice, matrix molar mass, additive molar mass, casting conditions, and chemistry of the TPU. Increases in matrix molecular weight or HBP core size, for example, would be expected to increase the driving forces for migration and phase separation but reduce the effective rates of diffusion [22]. The matrix selected here exhibited a very low T_g (−24 °C), resulting in room-temperature annealing, reducing the occurrence of kinetically trapped structures.

3.3. HBP–POM complex formation

The preceding results demonstrate that relatively low levels of substitution of perfluorinated and aliphatic chains are sufficient to induce surface segregation of the modified HBP in the TPU blends. The modified HPBs contain a number of unreacted amines that provide residual sites for the preparation of hybrid materials. HBP-based hybrid materials will likely exhibit similar segregation behavior and may be used to deliver species to the polymer surface at enhanced levels. Polyoxometalates (POMs) were identified as candidate materials to incorporate into the HBP structure. Their capabilities as mild oxidation catalysts are well documented [23] and the incorporation of POM catalysts onto polymer supports may have utility in certain applications. Additionally, their composition provides convenient and unambiguous spectroscopic characteristics to quantifiably measure their presence at a polymer surface. The specific POMs of interest were Keggin-type oxoanions with molecular formulae of $H_5PV_2Mo_{10}O_{40}$ (H_5POM) and $Na_5PV_2Mo_{10}O_{40}$ (Na_5POM). These and related POMs have been shown to degrade chemical warfare agents [24], and the thermoplastic polyurethanes support is a convenient model matrix for polymer coating or fabric systems.

The HBP was envisioned to interact with the POM as a ligand for the molybdenum/vanadium. Alternatively, PEIs are known to form polycation species, which could be used to displace the existing countercation of the POM, generating ion-paired species by forming the ammonium salt with the POM. Both routes of HBP–POM interaction were evaluated. Two solutions of HBP **5** were prepared in THF; one contained only the HBP and the other contained the HBP and 1 equiv of 1.0 M HCl (based on the total amine content of the PEI backbone, HBP **5**–H^+). The HBP solutions were then combined with the desired POM dissolved in the appropriate solvent. Mixing solutions of the POM (either H_5 or Na_5) and HBP **5** resulted in the immediate formation of a green precipitate that proved insoluble in all common solvents. Upon the addition of a stoichiometric amount of acid, the green precipitates dissolved, forming homogeneous solutions. No precipitate formed if the solution of HBP **5**–H^+ was used. The final H_5POM/Na_5POM–HBP **5**–H^+ complexes were light yellow solutions; the initial POMs appeared reddish (H_5POM) or orange (Na_5POM). The color change indicated the formation of different charge transfer complexes in the metalates due to interaction with the polyammonium species.

The electrostatic mechanism of interaction for the molybdenum-based POM is supported by FT-IR analysis of the HBP–POM complex. Films of HBP, POM, and the HBP–POM complex were cast on salt plates and then subjected to infrared absorption spectroscopy. Selected peaks of these spectra are shown in Fig. 4, and more are indicated in Table 3. It is known that the molybdenum–oxygen bond exhibits absorption in the IR region, and it has been used in this instance to evaluate the polyoxometalates and their complexes with the HBP. Polycrystalline MoO_4 with countercations exhibits absorptions ranging from ca. 750 cm^{-1} to 900 cm^{-1} [25]. The POMs demonstrated several signals within this range, ostensibly influenced by the

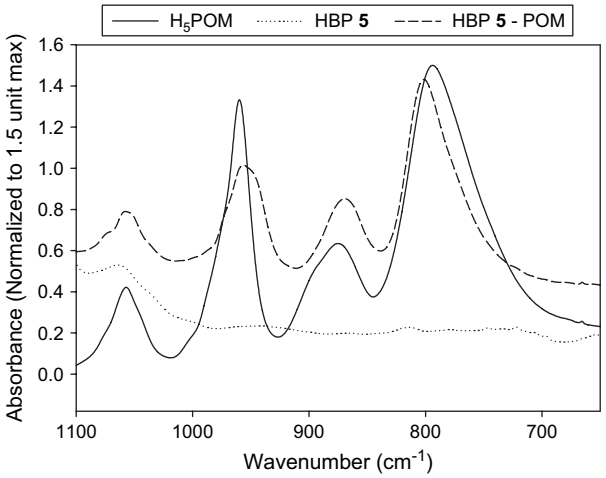

Fig. 4. IR spectra of POM absorbance. Spectral window shows absence of HBP absorption in the region of 1000–700 cm^{-1}, along with the H_5POM and its complex with the HBP. The subtle shifts in the peaks indicate a change in Mo oxoanion association, changing from the proton to the polycationic ammonium backbone of the PEI.

countercation of the POM. The H_5POM species had an absorption maximum at ca. 792 cm^{-1} and the sodium species exhibited an analogous maximum at ca. 784 cm^{-1}. Upon complexation with the protonated HBP, the complex exhibited an absorption peak at ca. 800 cm^{-1} regardless of the initial countercation. The collapse of the absorption peak indicates that the HBP has displaced the sodium or proton and is now acting as the countercation for the POM. Note that the other peaks listed in Table 3 also shift slightly. While the POMs are known to be most stable at acidic pH, the interior of the PEI is a basic environment. HBP–POM complexes were prepared from both a neutral HBP **5** solution (acidified after POM addition) and a polycationic HBP **5**–H^+ solution. The spectra of the HBP–POM complexes were nearly identical, indicating that the POM was stable until the polycation species formed. The consistency of the IR absorptions and their independence with respect to initial cation indicate the prominence of the ammonium salt as the determining interaction.

3.4. Surface characterization

POM–HBP hybrid materials were blended with the TPU matrix in THF and films were cast from homogeneous solutions. The surface properties of the resulting films were studied using contact angle analysis, AR-XPS, and RBS. A series of three compositions were prepared for both the sodium (**IV–VI**) and protic (**I–III**) metal oxides (see Fig. 5 for representative structure and Table 4 for compositions). The POM was maintained constant at 1% wt/wt relative to the TPU matrix, and the relative loading of the modified HBP **5** was varied as indicated in the table. The influence of the HBP–POMs on contact angle is consistent with the trend observed using the modified HBP **5** as an additive, where the HBP **5** increased the hydrophilicity of the surface of the TPU at low loading. Here the change in contact angle is greater, because the HBP is now in a polycationic form, generating a larger increase in surface energy. The ammonium salt backbone of the complex is sufficiently hydrophilic to dominate the surface chemistry of blends incorporating the protonated HBP, resulting in higher surface energy substrates.

While the contact angle data are useful for demonstrating that the HBP was present at the surface of the film, the analysis can provide no data about the distribution of metal in the sample. For that information AR-XPS and RBS were employed to interrogate the surface of the films. The AR-XPS results, shown in Table 5, provide compositional information for the top ca. 10 nm of the surface of the film. The fluorine concentration of samples doped with the hyperbranched additive increased as the take-off angle became shallower. A small amount of metal was also observed at the surface, primarily molybdenum with trace amounts of vanadium. These observations were consistent with the relative abundance of Mo and V for the POM, within experimental uncertainty. At 1% loading by weight, the average elemental abundance of Mo in the blend was less than 0.2% (atomic percentage). The observation of greater than 2% Mo, while still a small amount, indicates that the POM was transported to the surface effectively by the HBP.

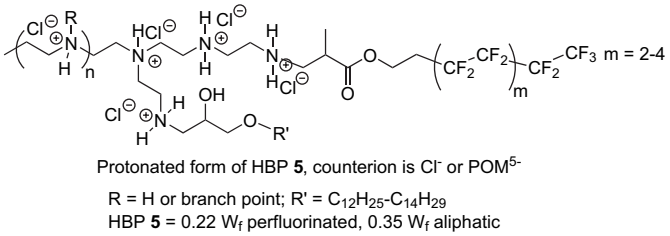

Fig. 5. Representative structure of polycation PEI, used to stabilize molybdenum-based POMs.

Table 3
IR absorption maxima of POM and POM–HBP complexes

Sample	H_5POM	Na_5POM	H_5POM + HBP **5**–H^+	Na_5POM + HBP **5**–H^+
Peak 1	792.5	783.9	801.9	799.1
Peak 2	870.8	862.7	870.2	868.3
Peak 3	958.4	948.2	952.8	949.5

Peak at 780–800 wavenumbers is indicative of shift in cation interaction. Peaks 1 and 3 show the greater dependence upon countercation, while peak 2 is weakly coupled to the change.

Table 4
Composition and contact angles for POM w/POM and HBP **5**–H^+

Sample	TPU equiv.	POM identity	POM equiv.	Prot. 5 equiv.	Adv. cont. ang.	Std. dev.
I	1.0	H_5POM	0.010	0.007	89.3	6.6
II	1.0	H_5POM	0.010	0.014	47.2	6.1
III	1.0	H_5POM	0.010	0.021	22.4	3.6
IV	1.0	Na_5POM	0.010	0.007	63.6	5.1
V	1.0	Na_5POM	0.010	0.014	19.6	1.5
VI	1.0	Na_5POM	0.010	0.021	23.9	1.6
HBP **5**–H^+	1.0	–	0.000	0.014	16.6	0.4

Contact angles determined from cast films of TPU w/1% wt/wt POM, with increasing quantities of HBP (0.7%, 1.4%, 2.1% by mass) across each series (**I–III**, **IV–VI**). Samples **I–III** were prepared with the H_5POM, while samples **IV–VI** were prepared with the Na_5POM. The final row indicates the performance of the protonated form of the HBP. The standard deviation of advancing contact angles is provided, as determined from at least five measurements.

Table 5
Atomic abundance of C, F, Mo at TPU–HBP–POM film surface determined via AR-XPS

Sample	90° TOA – atomic comp.				30° TOA – atomic comp.			
	C	F	Mo	O	C	F	Mo	O
POM + TPU	79.32	–	–	18.09	82.75	–	–	15.62
TPU + HBP **5**–H^+	64.28	13.52	–	9.59	68.23	12.90	–	7.84
I	61.61	10.31	2.90	24.02	60.54	17.48	2.34	18.33
II	61.65	14.51	2.31	19.11	60.25	22.18	1.99	13.30
III	62.11	16.56	1.73	16.26	60.14	23.56	1.54	11.82
IV	63.33	11.39	2.30	21.70	62.30	17.45	2.14	16.79
V	63.80	12.03	2.65	18.71	63.59	17.80	2.21	13.55
VI	63.61	13.49	2.10	19.09	58.66	24.10	1.94	13.68

Atomic abundance for C, F, Mo, O (normalized to 100% relative to all observed nuclei) at the stated take-off angle. Signal from nitrogen not integrated, as it overlapped with secondary Mo emissions. Films cast from TPU w/1% wt/wt POM, with increasing quantities of HBP (0.7%, 1.4%, 2.1% by mass) across each series (**I–III**, **IV–VI**). Samples **I–III** were prepared with the H_5POM, while samples **IV–VI** were prepared with the Na_5POM. The top column shows that no Mo was observed at the film surface in the absence of HBP, determined with 1% H_5POM.

The appearance of increased oxygen, when compared to protonated HBP **5** in TPU (second entry, Table 5), is also indicative of efficient POM surface transport. The blend containing protonated HBP in TPU (without POM) exhibited low oxygen content at the surface of the film (ca. 10%), whereas the films containing the protonated HBP–POM complex exhibited oxygen content near 20%. For each molybdenum atom, the POMs contained four oxygen atoms, so the increase in observed oxygen is further evidence of POM presentation at the surface, and confirms the relative abundance of Mo as between 2% and 3%.

The films were prepared with a constant amount of POM relative to TPU concentration (ca. 1% by mass), so the amount of hyperbranched polymer additive increased in each sample in the series. Consequently, the proportion of fluorine present at the surface increased across each series, which is reflected in the observed elemental abundance. As the quantity of HBP additive increased, the amount of POM appeared to remain constant or decrease slightly. The drop in observed oxygen content was offset by increases in the fluorine content (due to the increase of HBP concentration), while the level of molybdenum remained constant within the error of the instrument. The observation that the POM elemental concentration remained relatively constant suggests that the POM is saturating the available HBP, even at the highest level of HBP loading. This eventuality is not wholly unexpected, as the listed MW for the base PEI was only 1300 Da. The polymer backbone is therefore relatively small and compact, and likely cannot accommodate more than one POM cluster per HBP. Further experiments with higher MW PEIs have been planned and they may provide a more capable transport system for the presentation of POMs at a substrate surface.

Rutherford backscattering spectroscopy (RBS) provides a complementary technique to characterize the surface of the film for metal concentrations. The penetration depth of RBS permits measurement of the distribution of heavy nuclei further away from the polymer–air interface (ca. 2 μm for Mo). Depth resolution is dependent on the atomic number of the element of interest, and heavier nuclei allow resolution at increased depth. Fig. 6 shows the result of RBS results for three different polymer samples. The TPU was examined

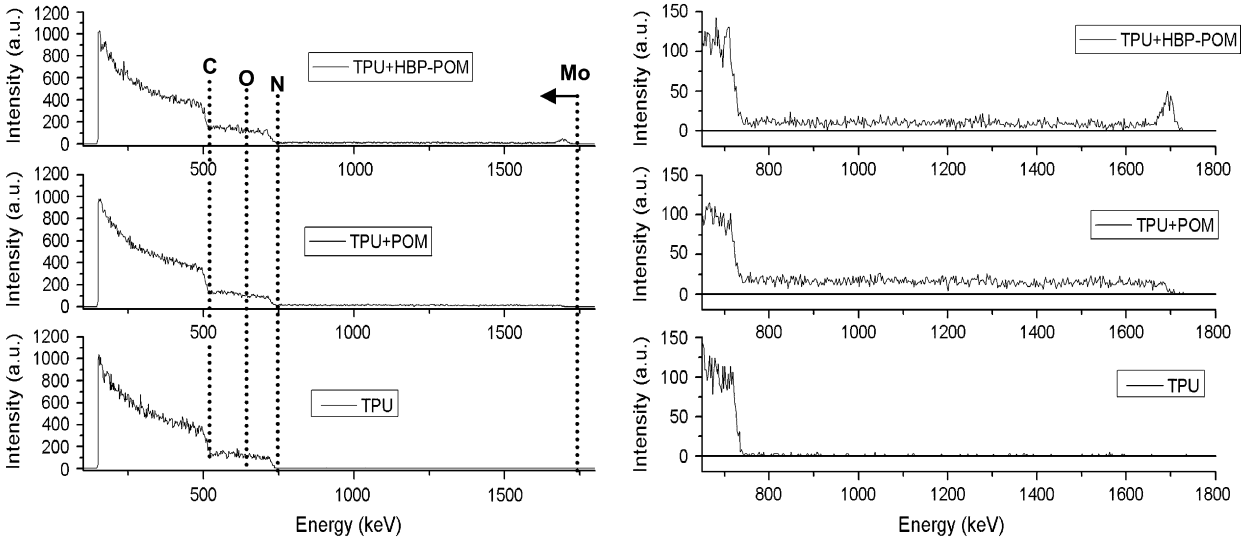

Fig. 6. RBS of HBP–POM complexes in TPU. The left plot shows the full scale RBS, which returns signal based on atomic number and concentration. As atomic number increases, the depth of resolution increases. The leading edge of the Mo signal provides resolution of about 2 μm until the N, O, C signals are observed. The plot at right expands the spectrum where the Mo is responsible for the signal, indicating noise only for the TPU, a uniform layer with the POM, and a surface enrichment for the HBP–POM complex (indicated by intensity increase at 1700 keV).

with no additive, as was one sample containing the TPU with H_5POM, and one sample with the corresponding HBP–POM complex. The long plateau of signal observed from ca. 800–1700 keV is the region where heavy nuclei scatter, and corresponds to a depth of resolution of ca. 2 μm. Molybdenum was the most populous heavy nucleus in the samples, and the signal from the 1% wt/wt loading can be clearly observed in the inset, when compared to the TPU control. The sample without HBP additive exhibits a uniform distribution of Mo throughout the sample. With the HBP–POM complex present, though, the concentration of Mo is increased near the film surface. The results indicate the presence of a Mo enriched layer ca. 50 nm thick with concentration of ca. 11-fold over the bulk loading amount (determined by analysis with the RUMP software) [19]. The increased surface concentration correlates well with the XPS results, and suggests that the HBP–POM conjugate preferentially segregates at the polymer surface.

The behavior exhibited by the films containing POM–HBP hybrids supports the conclusion that the additive is efficiently transported to the film surface. This transport phenomenon is dominated by the interplay of solvent evaporation and the relative solubilities of the matrix and additive in the film systems, and it is believed that this may enhance the surface transport of these additives. Further experiments are planned in thermoplastic systems to determine the utility of these additives in low-solvent and solvent-free environments.

4. Conclusions

Hyperbranched polyethyleneimines were functionalized with perfluorinated and aliphatic end groups, and were then combined with a thermoplastic polyurethane to generate a model film system. The resulting films exhibited changes in surface energy and surface composition, which scaled with the quantity of HBP and its level of end-group substitution. Surface migration of the HBPs was increased as a function of end-group substitution, but the hydrophilic PEI backbone resulted in increased surface hydrophilicity of the cast film. This trend was confirmed using AR-XPS, and provided elemental composition evidence that additive concentration near the surface was ca. 10-fold greater than that expected from the bulk concentrations. Similar increases were observed when hybrid complexes of the HBP and a polyoxometalate were prepared. Increased levels of molybdenum were observed at the surface, along with a corresponding elevation in surface oxygen content. The HBPs therefore transported the oxoanions to the substrate surface, enriching the concentration ca. 10-fold over the bulk level.

Acknowledgements

This research was supported in part through an appointment to the Postgraduate Research Participation Program at the U.S. Army Research Laboratory administered by the Oak Ridge Institute for Science and Education through an interagency agreement between the U.S. Department of Energy and USARL. It was also conducted with the support from the Strategic Environmental Research and Development Program (SERDP) project PP-1271. The authors would like to thank BASF, DuPont, and Resolution Performance Products for their generous donation of materials. Also, Dr. Heidi Schreuder-Gibson provided insight and helpful suggestions over the course of this work, and Eugene Napadensky was instrumental in the analysis of polymer molecular weights. Professor Craig Hill provided the polyoxometalates for this study.

References

[1] (A) Mason R, Jalbert CA, O'Rourke Muisener PAV, Koberstein JT, Elman JF, Long TE, et al. Adv Colloid Interface Sci 2001;94:1–19;
(B) O'Rourke Muisener PAV, Jalbert CA, Yuan C, Baetzold J, Mason R, Wong D, et al. Macromolecules 2003;36:2956–66.
[2] Walters KB, Schwark DW, Hirt DE. Langmuir 2003;19:5851–60.
[3] Suk DE, Chowdhury G, Matsuura T, Narbaitz RM, Santerre P, Pleizier G, et al. Macromolecules 2002;35:3017–21. Also see references cited therein.
[4] Lee MH, Fleischer CA, Morales AR, Koberstein JT, Koningsveld R. Polymer 2001;42:9163–72.
[5] Schacht PA, Koberstein JT. Polymer 2002;43:6527–34.
[6] Tanaka K, Kawaguchi D, Yokoe Y, Kajiyama T, Takahara A, Tasaki S. Polymer 2003;44:4171–7.
[7] Wang J, Kara S, Long TE, Ward TC. J Polym Sci Part A Polym Chem 2000;38:3742–50.
[8] Granville AM, Boyes SG, Akgun B, Foster MD, Brittain WJ. Macromolecules 2004;37:2790–6.
[9] Tomalia DA. Prog Polym Sci 2005;30:294–324.
[10] Voit B. J Polym Sci Part A Polym Chem 2005;43:2679–99.
[11] Gao C, Yan D. Prog Polym Sci 2004;29:183–275.
[12] (A) Krämer M, Stumbé J-F, Türk H, Krause S, Komp A, Delineau L, et al. Angew Chem Int Ed 2002;41:4252–6;
(B) Aulenta F, Hayes W, Rannard S. Eur Polym J 2003;39:1741–71.
[13] (A) Goetheer ELV, Baars MWPL, van den Broeke LJP, Meijer EW, Keurentjes JTF. Ind Eng Chem Res 2000;39:4634–40;
(B) Garcia-Berabé A, Krämer M, Olàh B, Haag R. Chem Eur J 2004;10:2822–30.
[14] Kim YH, Webster OW. Macromolecules 1992;25:5561–72.
[15] (A) Schmaljohann D, Pötschke P, Hässler R, Voit BI, Froehling PE, Mostert B, et al. Macromolecules 1999;32:6333–9;
(B) Huber T, Pötschke P, Pompe G, Hässler R, Voit B, Grutke S, et al. Macromol Mater Eng 2000;280/281:33–40.
[16] Orlicki JA, Thompson JL, Markoski LJ, Sill KN, Moore JS. J Polym Sci Part A Polym Chem 2002;40:936–46.
[17] (A) Hong Y, Cooper-White JJ, Mackey ME, Hawker CJ, Malmström E, Rehnberg N. J Rheol 1999;43:781–93;
(B) Hong Y, Coombs SJ, Cooper-White JJ, Mackay ME, Hawker CJ, Malmström E, et al. Polymer 2000;41:7705–13.
[18] Zeng H, Newkome GR, Hill CL. Angew Chem Int Ed 2000;39:1771–4.
[19] Doolittle LR. Nucl Instrum Methods 1986;B15:227.
[20] Wadsworth L, Sun CQ, Shang D, Zhao R, Schreuder-Gibson H, Gibson P. Proceedings of the international nonwovens technical conference; 2001.
[21] Tan H, Guo M, Du R, Xie X, Li J, Zhong Y, et al. Polymer 2004;45:1647–57.
[22] Baille WE, Malveau C, Zhu XX, Kim YH, Ford WT. Macromolecules 2003;36:839–47.
[23] (A) Sonnen DM, Reiner RS, Atalla RH, Weinetock IA. Ind Eng Chem Res 1997;36:4134–42;
(B) Xu L, Boring E, Hill CL. J Catal 2000;195:394–405.
[24] (A) Johnson RP, Hill CL. J Appl Toxicol 1999;19:S71–5;
(B) Boring E, Geletii YV, Hill CL. J Mol Catal A Chem 2001;176:49–63.
[25] (A) Hanuza J, Maczka M, Hermanowicz K, Dereń PJ, Strek W, Folcik L, et al. J Solid State Chem 1999;148:468–78;
(B) Maczka M, Hanuza J, Lutz ETG, van der Maas JH. J Solid State Chem 1999;145:751–6.